OFFICE OF NAVAL RESEARCH

GRANT N00014-89-J-1178

R&T CODE 413Q001-05

TECHNICAL REPORT NO. #57

APPLICATIONS OF IN-SITU ELLIPSOMETRY TO MICROWAVE ELECTRON CYCLOTRON RESONANCE PLASMA PROCESSES

Y.Z. Hu, J. Joseph and E.A. Irene
Department of Chemistry
University of North Carolina at Chapel Hill
Chapel Hill, NC 27599-3290

Submitted to:

Journal of Vacuum Science and Technology

REPORT DOCUMENTATION PAGE

Form Approved
OMB No 0704-0188

1. AGENCY USE ONLY (Leave blank)	2. REPORT DATE	3. REPORT TYPE AND DATES COVERED
	5/4/93	

4. TITLE AND SUBTITLE
Applications of In-Situ Ellipsometry to Microwave Electron Cyclotron Resonance Plasma Processes

5. FUNDING NUMBERS
#N00014-89-J-1178

6. AUTHOR(S)
Y.Z. Hu, J. Joseph and E.A. Irene

7. PERFORMING ORGANIZATION NAME(S) AND ADDRESS(ES)
The University of North Carolina
Chemistry Department
CB #3290 Venable Hall
Chapel Hill, NC 27599-3290

8. PERFORMING ORGANIZATION REPORT NUMBER
Technical Report #57

9. SPONSORING/MONITORING AGENCY NAME(S) AND ADDRESS(ES)
Office of Naval Research
800 N. Quincy Street
Arlington, VA 22217-5000

10. SPONSORING/MONITORING AGENCY REPORT NUMBER

11. SUPPLEMENTARY NOTES
None

12a. DISTRIBUTION/AVAILABILITY STATEMENT
This document has been approved for public release and sale, distribution of this document is unlimited.

12b. DISTRIBUTION CODE

13. ABSTRACT *(Maximum 200 words)*

In-situ static spectrosocpic ellipsometry used during a process is a powerful method for characterizing the optical properties and structure of multilayered thin films. However, the commonly practiced rotating element ellipsometry takes about 10 min for each spectral measurement. Using only a single wavelength gives less information, but each measurement time reduces to about 5 sec. It is shown that a combination of the techniques was adequate to investigate the plasma processes. Spectroscopic ellipsometry, SE, measurements for Si, Ge, InP, InSb and GaAs showed that for properly selected photon energy ranges, the dependence of the dielectric functions on temperature is minimum while the sensitivity to surface modifications is high. The ECR plasma oxidation of Si is discussed first, since it is the simplest case, and then attention is given to more complex example of ECR plasma ion bombardment induced oxidation and damage in single crystal Ge.

14. SUBJECT TERMS
Plasma, insitu static

15. NUMBER OF PAGES

16. PRICE CODE

17. SECURITY CLASSIFICATION OF REPORT	18. SECURITY CLASSIFICATION OF THIS PAGE	19. SECURITY CLASSIFICATION OF ABSTRACT	20. LIMITATION OF ABSTRACT
Unclassified	Unclassified	Unclassified	

Presented at 39th AVS, Nov.7-13, Chicago. Submitted to JVST 1992.

APPLICATIONS OF IN-SITU ELLIPSOMETRY TO MICROWAVE ELECTRON CYCLOTRON RESONANCE PLASMA PROCESSES

Y.Z. Hu, J. Joseph and E.A. Irene
Department of Chemistry, CB# 3290
University of North Carolina
Chapel Hill, NC 27599-3290

ABSTRACT

In-situ static spectroscopic ellipsometry used during a process is a powerful method for characterizing the optical properties and structure of multilayered thin films. However, the commonly practised rotating element ellipsometry takes about 10 min for each spectral measurement. Using only a single wavelength gives less information, but each measurement time reduces to about 5 sec. It is shown that a combination of the techniques was adequate to investigate the plasma processes. Spectroscopic ellipsometry, SE, measurements for Si, Ge, InP, InSb and GaAs showed that for properly selected photon energy ranges, the dependence of the dielectric functions on temperature is minimum while the sensitivity to surface modifications is high. The ECR plasma oxidation of Si is discussed first, since it is the simplest case, and then attention is given to more complex example of ECR plasma ion bombardment induced oxidation and damage in single crystal Ge.

I. INTRODUCTION

Advantages of the microwave electron cyclotron resonance, ECR, plasmas include electrodeless operation which reduces wall contamination, low plasma potential which reduces ion-induced surface damage, high plasma density, and low pressure operation, which produces high etch rates with low particulate formation[1]. In ECR systems the high etching and deposition rates achieved are indirect evidence of the high efficiency of ECR plasmas[2,3]. The microelectronics process industry is moving towards adopting the concept of "single wafer processing". This concept embodies the use of ECR plasma process chambers in which one or several process steps such as cleaning, film deposition, etching, annealing, etc. are to be carried out. Since one wafer at a time is processed, it is quite clear that in-situ process monitoring is required that is non destructive, non-invasive, i.e. the monitor does not alter the process, and that sufficient process information can be accessed by the technique. Spectroscopic ellipsometry (SE) is particularly attractive, as it has submonolayer sensitivity and in its spectroscopic form [4] has evolved into a formidable diagnostic tool for nondestructively analyzing thin films[5,6,7]. Single wavelength ellipsometers employing available gas-laser sources have already demonstrated good sensitivity in monitoring the vapor phase epitaxial growth of AlGaAs[8] and Si[9]. The literature[10,11,12] shows that the diagnostic power of ellipsometry can be greatly enhanced with a properly selected wavelength. The purpose of this study is to demonstrate the suitability of automated, in-situ ellipsometry for ECR plasma process monitoring. In our laboratory the applications of ellipsometry have included ion beam damage[12,13], ion beam cleaning[14,15], ECR plasma oxidation of Si[16,17], and ECR plasma CVD[18]. Information has been extracted on the evolution of film thicknesses and optical properties, including information about surface roughness and damage layers. As

examples, this paper uses real time single wavelength ellipsometry to measure the growth kinetics, along with in-situ spectroscopic ellipsometry to characterize the surface layer structures during the ECR oxygen plasma bombardment of Si and Ge substrates.

II. EXPERIMENTAL PROCEDURES

The experimental system was described previously[17]. The spectroscopic ellipsometer used for this study was designed and constructed in our laboratory[19,20]. It is similar in design to the polarizer-sample-rotating analyzer system described by Aspnes[21]. A 75 watt Xenon arc lamp serves as the broad band (200-800 nm) light source, and the monochromator is positioned after the analyzer to allow background light subtraction in high background ambients such as plasmas or for high temperature processing. The reflected light obtained at the rotating analyzer exit is periodic in intensity and of the following form:

$$I = A_0[\,1 + A_2\cos 2\theta + B_2\sin 2\theta\,] \tag{1}$$

where A_2 and B_2 are second-order Fourier coefficients. The ellipsometric parameters Ψ and Δ are related to A_2 and B_2 through the following expressions:

$$\tan\psi = \tan P\sqrt{\frac{1+A_2}{1-A_2}} \qquad \cos\Delta = \frac{B_2}{\sqrt{1-A_2^2}} \tag{2}$$

where P is the polarizer azimuth angle. Spectroscopic ellipsometry measures the complex reflectance ratio ρ given as:

$$\rho = \frac{r_p}{r_s} = \tan\psi e^{i\Delta} \tag{3}$$

where the reflection coefficients r_p and r_s are for light polarized parallel (p) and perpendicular (s) to the plane of incidence. In the case of a pure material without any surface overlayer, ρ is directly related to the dielectric function ε of the material through the relation:

$$\varepsilon = \varepsilon_1 - i\varepsilon_2 = \sin^2\phi_0\left[\,1 + \tan^2\phi_0\left(\frac{1-\rho}{1+\rho}\right)^2\right] \tag{4}$$

where ϕ_0 is the angle of incidence (70^0 in the present experiment). In general, equation (4) yields a pseudo dielectric function, because overlayer films are invariably present on the

substrate. The ellipsometric measurements do not determine sample properties themselves, but these data can be related to sample properties through well-defined model calculations using the Bruggeman effective medium approximation[22], BEMA. In this approximation the effective-medium dielectric function ε is given by:

$$0 = \sum_{i=1}^{n} f_i \frac{\varepsilon_i - \varepsilon}{\varepsilon_i + 2\varepsilon} \tag{5}$$

where n is the number of distinct constituent media in the mixture, f_i is the volume fraction of the ith component, ε_i is the dielectric function of the i^{th} component. For a multilayer system, the set of equations comprising the model can be written schematically as:

$$\rho = \rho(\varepsilon_s; \varepsilon_j; L_j; \varepsilon_a; \phi; \lambda) \tag{6}$$

where ε_s, ε_j and ε_a are the dielectric functions of the substrate, the different layers, and the ambient, respectively, the L_j are the layer thicknesses, ϕ is the angle of incidence, and λ is the wavelength. From a literature database for the known constituents of the film and substrate ρ_{cal} is calculated and compared with ρ_{exp}
and as a figure of merit for comparison, an unbiased estimator δ is calculated from the relationship[23]

$$\delta = \left[\frac{1}{N-P-1} \sum_{i=1}^{n} (\varepsilon_{exp} - \varepsilon_{cal})^2 \right]^{1/2} \tag{7}$$

where N is the number of wavelengths and P the number of unknown parameters. A minimizing procedure gives the best fit parameters which are film thicknesses and percents of constituents at the 90% confidence level.

III. RESULTS AND DISCUSSION

1. Single Wavelength Ellipsometry Real Time Measurements

Spectroscopic ellipsometry using rotating elements is widely used for analysis of complex multilayer structures, but with the use of scanning monochromators the time for acquisition of a spectrum is about 10-20 min in our case. Recently rapid scan spectroscopic ellipsometry has been reported using detector arrays[24]. Single wavelength ellipsometry can be used for real time measurement (about 5 second for each measurement in our case), but only for well characterized systems. However, a combination of single wavelength and SE is shown to provide substantive information about processes. In order to chose an appropriate single wavelength for a process, several factors must be considered. First, the dielectric function of most substrate materials is temperature dependent. Figure 1 shows the floating temperature attained by Si wafers in different gas ECR plasmas, which confirms that optical properties must be known as a function of temperature. Fortunately, for most semiconductor

materials there is a photon energy regime in which the optical properties (the complex refractive index or the complex dielectric function) are relatively insensitive to temperature. We have measured the dielectric function at different temperatures for Si, Ge, InP and InSb and present our results in Fig.2. Jellison[25] and Aspnes[26] reported similar results for Si and GaAs, respectively. On the other hand, the wavelengths that are sensitive to temperature from Fig.2 can be used to monitor the wafer temperature[27]. Second, the ellipsometric angle values of Ψ and Δ must be in a region where the accuracy of the rotating analyzer ellipsometer is good. Third, there must be high sensitivity to the thickness variation of the films studied. Fourth, at the photon energy chosen the transparency of the top layer must be high and low for the substrate, i.e. the materials must be optically dissimilar, but in the correct order.

2. ECR Plasma Oxidation of Si

As a simple example, the results of the ECR plasma oxidation of Si are discussed. It was previously shown[17] using SE, that during the ECR oxidation of Si the top SiO_2 layer grows with an almost constant interface layer underneath. Therefore, it is straightforward to measure the film growth by single wavelength ellipsometry. The wavelength used was 340 nm (3.65 eV). Figure 3a gives the measured Δ and Ψ values for the oxidation. In order to interpret the single wavelength measurements in terms of oxidation kinetics, a trajectory method was used[28]. For this calculation the refractive index of the substrate is calculated from the first experimental point (at 400 °C), and using this value a trajectory in the Δ and Ψ plane corresponding to the growth of the layer with an arbitrary index is compared to the experimental points. For the comparison an error function is defined as the sum of the distance between the experimental points and the calculated trajectory in the Δ and Ψ plane. With the use of a minimization procedure the index of the layer is varied to obtain the minimum of the error function. In Fig.3a the solid line corresponds to a calculation performed with a one layer model with an index n=1.478. The evolution of the oxide film thicknesses as a function of the oxidation time is obtained by the trajectory method and shown in Fig.3b as the solid line. From this procedure and using a measured refractive index for the starting cleaned Si surface at room temperature the thickness evolution is obtained as the dashed line in Fig.3b. From Fig.3b, we obtained the thicknesses of 28.0 and 28.4 nm at oxidation time of 80 min for room temperature and the 400 °C substrate index, respectively. After oxidation and cooling to room temperature, the SE, shown in Fig.3c, was obtained. The total thickness from SE is 28.6 nm which is excellent agreement with single wavelength measurement at 400 °C. The inset in Fig.3c shows the two layer model used for the fit (solid line) from which the thickness values are obtained.

3. ECR Oxygen Plasma Ion Bombardment of Ge

The goal of this experiment is to understand the structural changes that occur in a Ge surface caused by low energy and high dose oxygen ion bombardment in an ECR plasma, and the dependence of the surface modification on ion energy. This information is of practical interest because high dose implanted oxygen layers in Ge, give low reflectivity in the far-UV and visible, and are thus promising materials for efficiently absorbing photons for photodetectors and solar energy converters[29,30]. We have demonstrated from our ECR

plasma experiments[31] that the square of the ion current, I_i^2, increases approximately linearly with negative bias, V_b, of the sample holder. A measurement of I_i^2 vs $-V_b$ (up to -1000 V) in the oxygen plasma at $5x10^{-4}$ Torr shows that an ion dose rate of about $5x10^{15}$ ions/sec.cm^2 can be obtained from the down stream ECR plasma. A combination of real time single wavelength ellipsometry and in-situ spectroscopic ellipsometry was used to monitor the changes in the surface during oxygen ion bombardment, to determine the ion bombardment saturation point, and to give the surface layer structure and composition after ion bombardment. We used 335 nm for the real time single wavelength ellipsometry measurement, because at this wavelength the measurement is both temperature insensitive and surface modification sensitive. The dependence of Δ and Ψ on the duration of oxygen ion bombardment of Ge indicates that after a rapid initial change, the Δ and Ψ values change very slowly with increasing exposure time then saturated. Figure 4 gives a typical Δ vs bombardment time at different ion energies. The saturation behavior is believed due to the competing effects of deposition and sputtering, where an equilibrium is reached for some film thickness value. In order to determine the sputter etch effect, we measured two Ge samples with about 10-15 nm oxide film on top at -300 and -60 V using both SE and single wavelength ellipsometry, and with the single wavelength results shown in Fig.5a and 5b, and SE results in 5c. For the bias of -300 V the etch rate is too fast to use spectroscopic measurement.

The SE results in Fig.6a show that it is likely that damage increases for the higher negative biases. In order to interpret the SE results four sensible models, similar to those in our previous paper[17], were evaluated. A two layer model, with pure GeO_2 as the topmost layer and with a damage layer composed of GeO_2 and a-Ge underneath always yielded the best fit in terms of the lowest unbiased estimator δ. A comparison of the results from the best fit model for the five bias values in 6a is shown in Fig.6b. It is seen that both the pure oxide top layer and the damage layer increase with increasing ion bombardment energy. It is interesting to observe from Fig.6b that the composition of the damage layer is not dependent on the ion energy. The best fit optical models of SE data were independently checked by angle resolved x-ray photoelectron spectroscopy, XPS. The XPS Ge 3d spectra show only presence of a pure GeO_2 layer on top with a peak in binding energy near 33.5 eV (for thermal GeO_2), without a free Ge peak at 29.4 eV. The total oxide thickness can also be determined from XPS measurement and is shown in Table 1.

IV. CONCLUSIONS

(1) Combining in-situ SE with real time single wavelength ellipsometry, at an appropriate single wavelength, yields considerable information about ECR plasma processes.

(2) For the common semiconductor materials: Si, Ge, InP, InSb and GaAs, there are some special wavelengths or ranges in which the dielectric functions are insensitive or highly sensitive to temperature.

(3) Using the temperature insensitive wavelength of 340 nm for ECR oxidation of Si, the real time measurement at 400 ^{o}C gives the oxide thickness comparable to values measured after cooling the sample to room temperature and with SE measurements.

(4) ECR plasma oxygen ion bombardment of single crystal Ge caused complex surface modifications. From SE measurements the surface growth film is composed of two layers:

a pure GeO_2 layer and a damage layer. Optically, the damage layer is composed of 65% a-Ge and 35% GeO_2 which is independent of ion energy.

ACKNOWLEDGMENTS

This work was supported in part by the National Science Foundation, NSF, and the Office of Naval Research, ONR.

REFERENCES

1. J.E. Stevens, J.L. Cecchi, Y.C. Huang and R.L. Jarecki,Jr, J. Vac. Sci. Technol. A9, 696 (1991).
2. K. Kobayashi, M.Hayama, S.Kawamoto, and J. Miki, Jpn. J. Appl. Phys., 26, 202 (1987).
3. S. Matsuo, Vacuum, 31, 279 (1988).
4. D.E.Aspnes, in Optical Properties of Solids; New Developments, edited by B.O.Seraphin (North-Holland, Amsterdam, 1976), P.799.
5. D.E.Aspnes, W.E. Quinn, and S. Gregory, Appl. Phys. Lett., 56, 2569 (1990).
6. R.W. Collins, J. Vac. Sci. Technol. A, 7, 1378 (1989).
7. R.W. Collins, Rev. Sci. Instrum., 61, 2069 (1990).
8. F. Hottier and G. Laurence, Appl. Phys. Lett., 38, 863 (1981).
9. C.Peckering, D.J. Robbins, I.M. Young, J.L. Glasper, M. Johnson, and R. Jones, Mater. Res. Soc. Symp. Proc., 94, 173 (1987).
10. B. Drevillon, Thin Solid Films, 163, 157 (1988).
11. R. W. Collins and B.Y. Yang, J. Vac. Sci. Technol. B, 7, 1155 (1989).
12. Y.Z.Hu, J.W.Andrews, M.Li and E.A. Irene, Nucl. Instr. Meth., B59/60, 76 (1991).
13. Y.Z. HU, M. Li, K. Conrad, J.W.Andrews, E.A. Irene, M. Denker, M. Ray and G. McGuire, J. Vac. Sci. Technol. B, 10, 1111 (1992).
14. Y.Z. Hu, K.A. Conrad, M. Li, J.W. Andrews, J.P. Simko and E.A. Irene, Appl. Phys. Lett., 58, 589 (1991).
15. Y.Z. Hu, M. Li, J.W. Andrews, K.A. Conrad and E.A. Irene, J. Electrochem. Soc., 139, 2022 (1992).
16. Y.Z. Hu, J. Joseph and E.A. Irene, Appl. Phys. Lett., 59, 1353 (1991).
17. J. Joseph, Y.Z. Hu and E.A. Irene, J. Vac. Sci. Technol. B 10, 611 (1992).
18. M.Li, Y.Z. Hu, K.A. Conrad and E.A. Irene, (This meeting).
19. J.W. Andrews, Y.Z. Hu and E.A. Irene, SPIE Proceedings of Multichannel and In-Situ Processing of Electronic Materials, 1188, 162 (1989).
20. J.W. Andrews, Ph.D thesis, University of North Carolina, Chapel Hill, NC 1990.
21. D.E.Aspnes and A.A. Studna, Rev. Sci, Instrum., 49, 291 (1978).
22. D.E. Aspnes, Thin Solid Film, 89, 249 (1982).
23. D.E.Aspnes, J.B. Theeten, and F. Hottier, Phys. Rev. B 20, 3992, (1979).
24. I. An and R.W. Collins, Rev. Sci. Instr., 62, 1904 (1991).
25. G.E. Jellison, Jr and F.A. Modine, Physical Review B, 27, 7466 (1983).
26. D.E. Aspnes, W.E. Quinn, and S. Gregory, Appl. Phys. Lett., 56, 2569 (1990).
27. K.A. Conrad, R.K. Sampson, H.Z. Massoud and E.A. Irene, submitted to J. Vac. Sci. Technol. B.

28. A.Gagnaire, J.Joseph and A. Etcheberry, J. Electrochem. Soc. 134, 2476 (1987).
29. Q.C. Zhang, J.C. Kelly and M.J. Kenny, Nucl. Instr. and Meth., B47, 257 (1990).
30. N.M. Ravindra, T.Fink, W. Savin, T.P.Sjoreen, R.L. Pfeffer, L.G. Yerke, R.T. Lareau, J.G. Gualtieri and R. Lux and C. Wrenn, Nucl. Instr. and Meth., B46, 409 (1990).
31. Y.Z. Hu, M. Li, J.P. Simko, J.W. Andrews, and E.A. Irene, in "Proceedings of the Eleventh International Conference on CVD", edited by k.E.Spear and G.W.Cullen, (The Electrochemical Society, Pennington, N.J., 1990).

FIGURE CAPTIONS

Figure 1. The floating temperature of Si wafers in different gas ECR plasmas at $5x10^{-4}$ Torr and 300 W.

Figure 2. Pseudodielectric functions of Si, Ge, InP and InSb at different temperatures.

Figure 3. Typical ellipsometry results from the ECR oxidation of Si at 400°C, 450W and +60 V bias. a. Evolution of Δ and Ψ trajectories during oxide growth at a wavelength of 340 nm. The solid line corresponds to an one layer model calculation with index of n=1.478; b. Thicknesses of the grown oxide layer vs oxidation time, calculated from the substrate index data at room temperature (dashed) and 400°C (solid); c. Spectroscopic ellipsometry measurement and the optical model after 80 min oxidation.

Fig. 4. Typical Δ vs time during ECR oxygen plasma ion bombardment of Ge at various substrate bias values.

Fig. 5. ECR oxygen plasma ion etching of GeO_2. a. Evolution of Δ and Ψ trajectories during etching at a wavelength of 335 nm. The solid line corresponds to an one layer model calculation with index of n=1.72; b. Etch rate at -300 V, measured by single wavelength ellipsometry; c. Etch rate at -60 V, measured by SE.

Figure 6. Pseudodielectric function spectra and the optical models of single crystal Ge after saturation bombardment with oxygen plasma ions at different ion energies.

TABLE CAPTIONS

Table 1 Total oxide thicknesses induced by plasma oxygen ion bombardment on Ge, measured by XPS and SE.

Table 1 Total oxide thicknesses induced by plasma oxygen ion bombardment on Ge, measured by XPS and SE

Conditions	θ	$I_m(3d)$	$I_\infty(3d)$	λ	L_{XPS}	L_{SE}
-1000 V	40°	200	38610	28 nm	11.1 nm	
Saturation bombardment	70°	1199	36273	28 nm	10.5 nm	10.1 nm

* Thickness $L_{XPS} = \lambda \sin\theta \ln(I_M/I_\infty)$

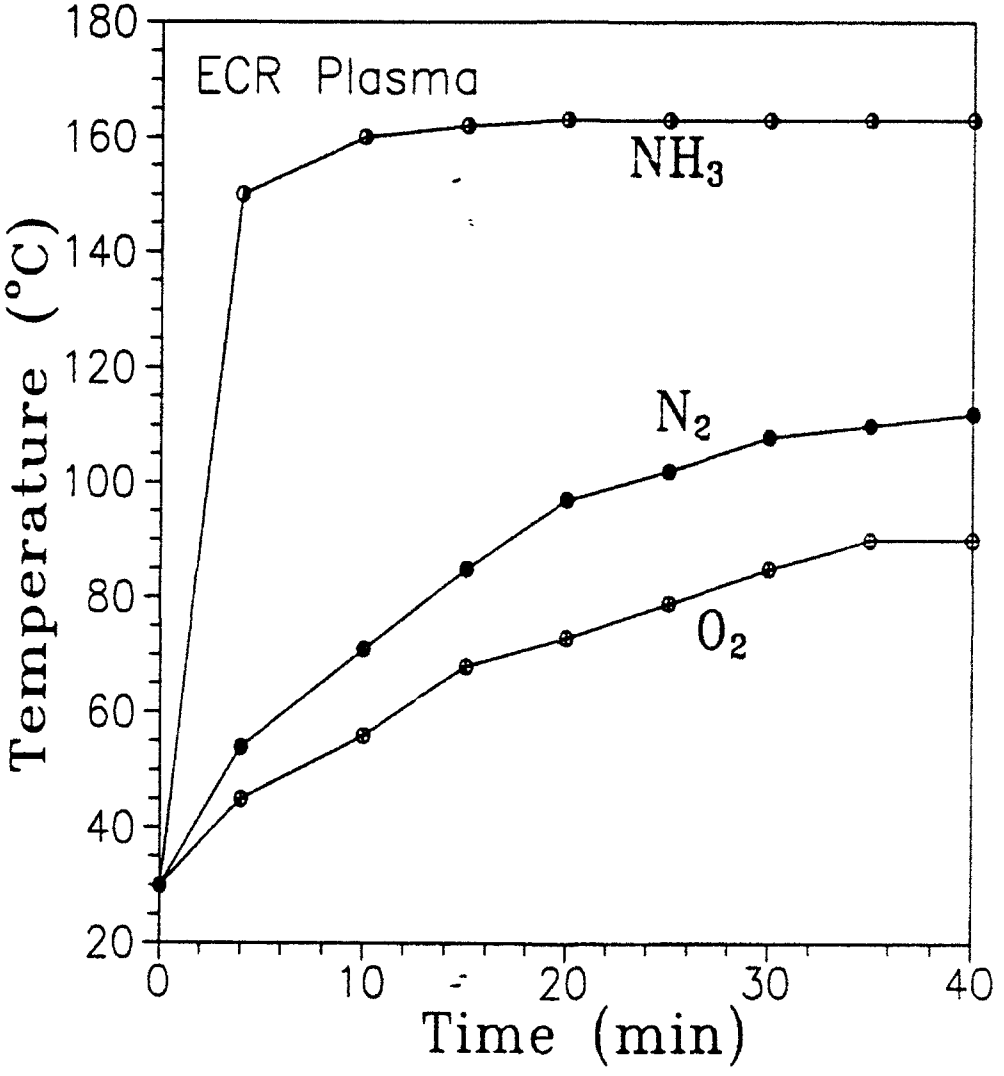
ECR Plasma
NH_3
N_2
O_2
Temperature (°C)
Time (min)
180
160
140
120
100
80
60
40
20
0
10
20
30
40

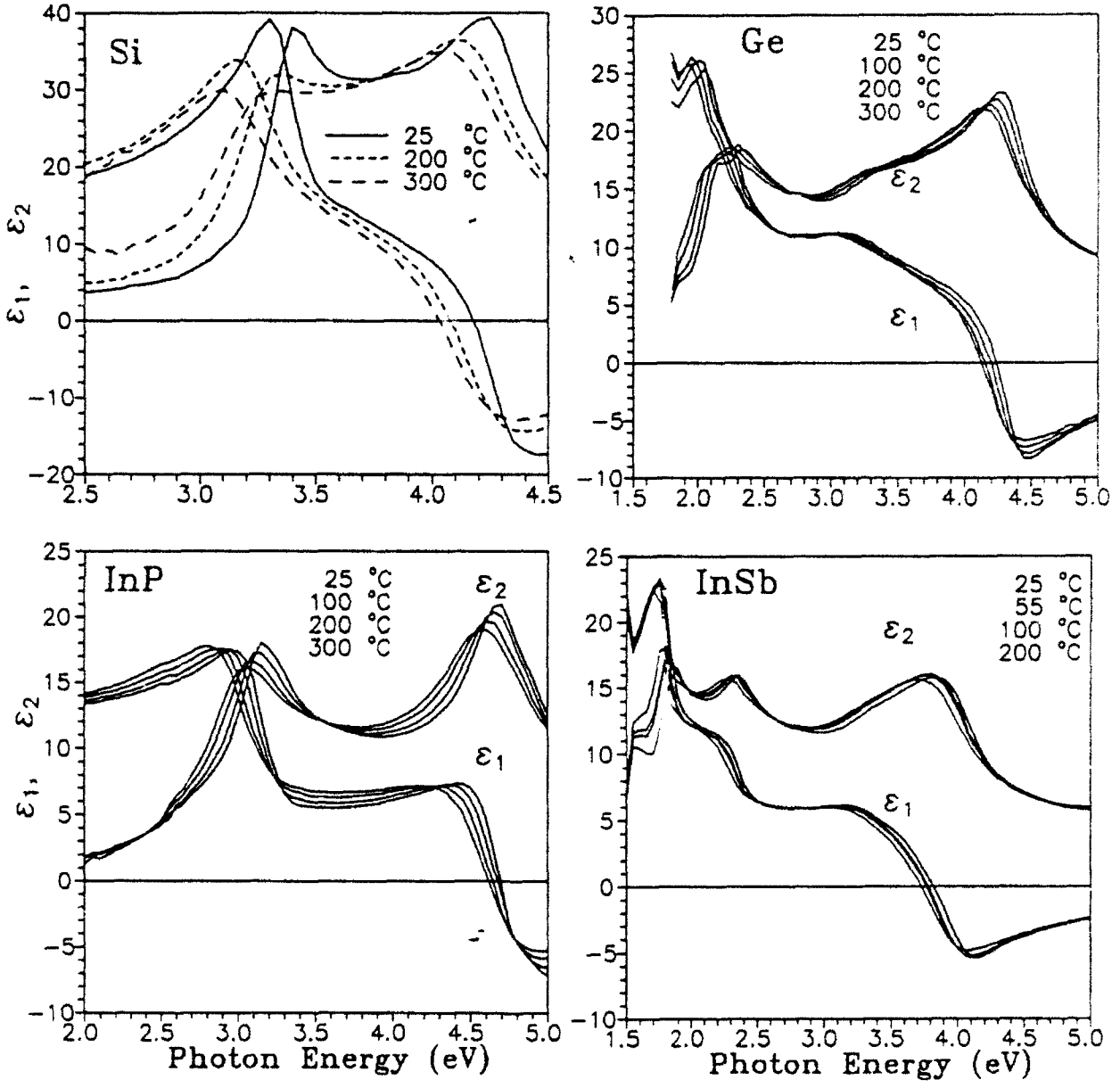
Si
25 °C
200 °C
300 °C
ε1, ε2
Ge
25 °C
100 °C
200 °C
300 °C
ε2
ε1
InP
25 °C
100 °C
200 °C
300 °C
ε2
ε1
ε1, ε2
Photon Energy (eV)
InSb
25 °C
55 °C
100 °C
200 °C
ε2
ε1
Photon Energy (eV)

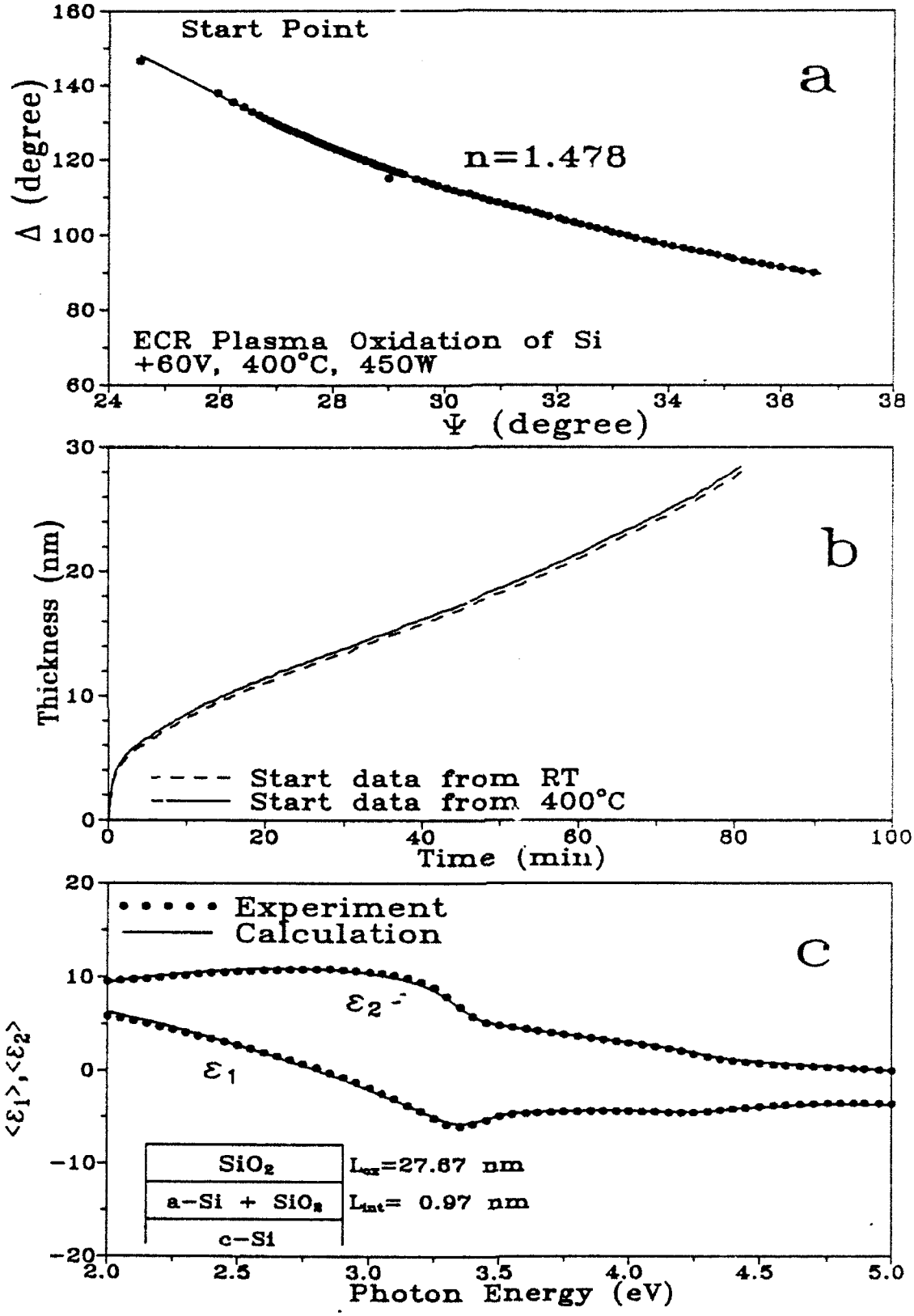
Start Point
a
n=1.478
ECR Plasma Oxidation of Si
+60V, 400°C, 450W
Δ (degree)
Ψ (degree)
b
Thickness (nm)
Start data from RT
Start data from 400°C
Time (min)
Experiment
Calculation
c
ε2
ε1
<ε1>,<ε2>
SiO2
a-Si + SiO2
c-Si
Lox=27.67 nm
Lint= 0.97 nm
Photon Energy (eV)

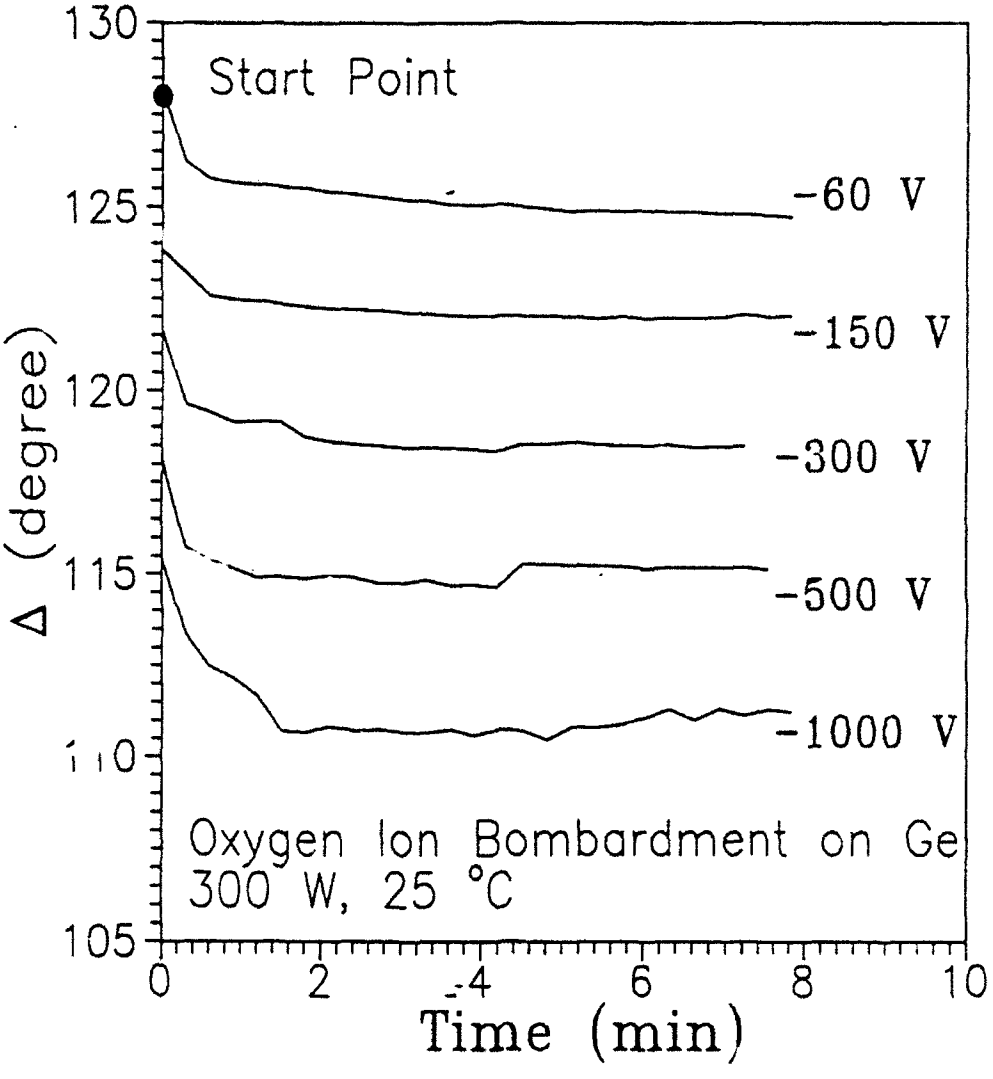
130
125
120
115
110
105
Δ (degree)
Start Point
-60 V
-150 V
-300 V
-500 V
-1000 V
Oxygen Ion Bombardment on Ge
300 W, 25 °C
0
2
4
6
8
10
Time (min)

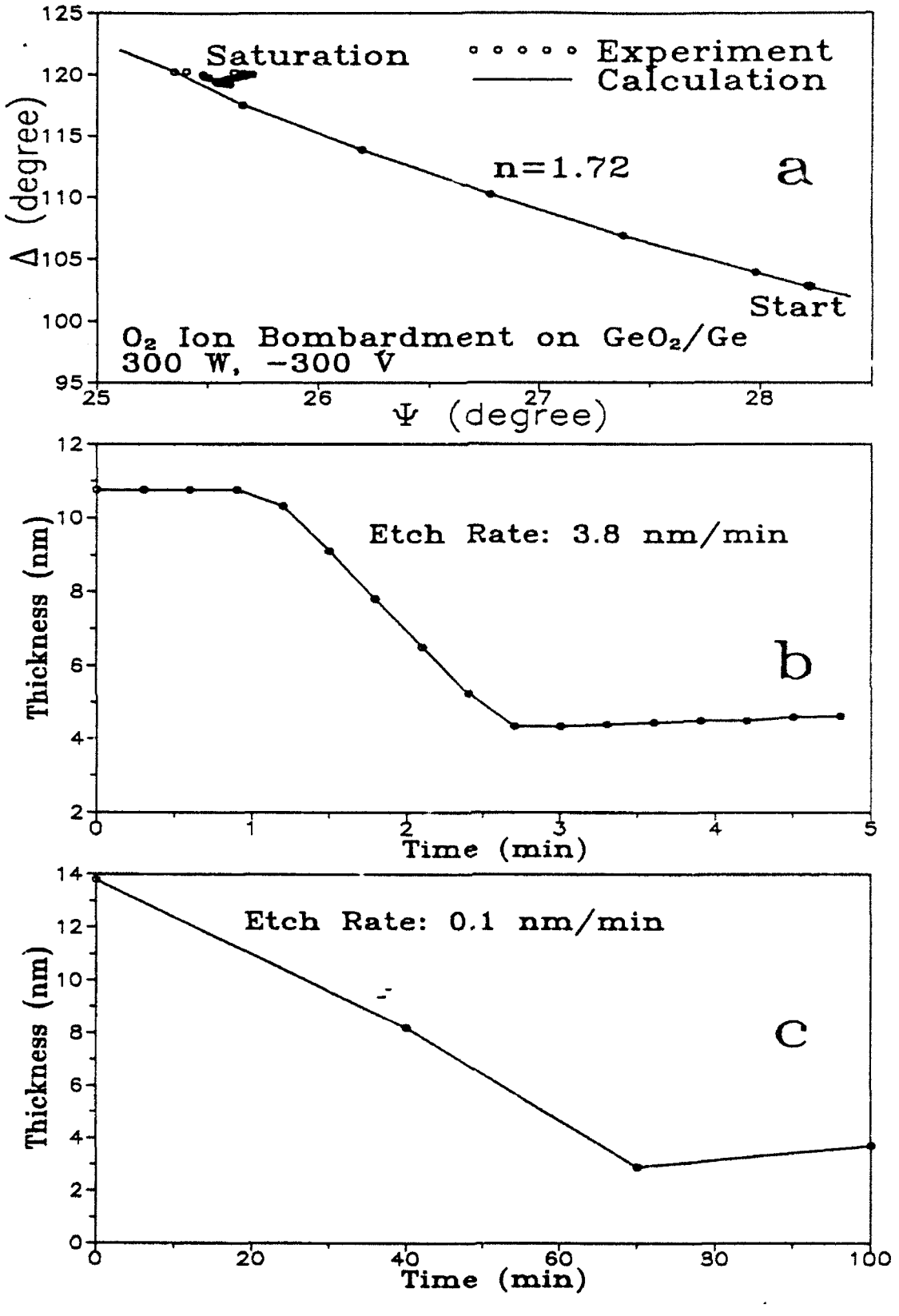
Saturation
Experiment
Calculation
n=1.72
a
Start
O2 Ion Bombardment on GeO2/Ge
300 W, -300 V
Δ (degree)
Ψ (degree)
Etch Rate: 3.8 nm/min
b
Thickness (nm)
Time (min)
Etch Rate: 0.1 nm/min
c
Thickness (nm)
Time (min)

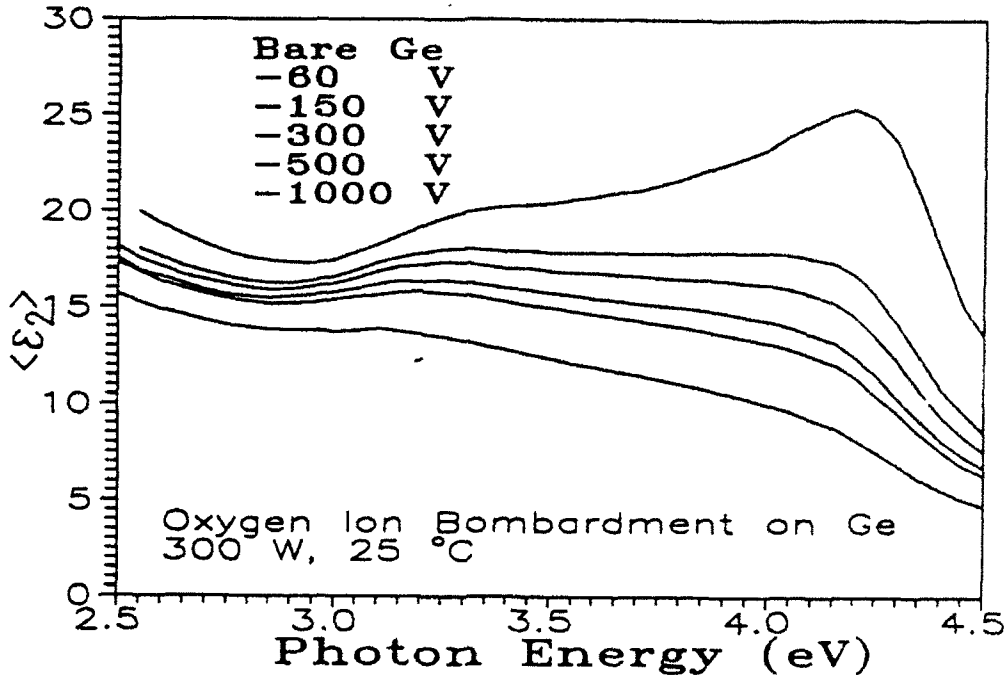
Bare Ge
−60 V
−150 V
−300 V
−500 V
−1000 V
Oxygen Ion Bombardment on Ge
300 W, 25 °C
<ε2>
Photon Energy (eV)

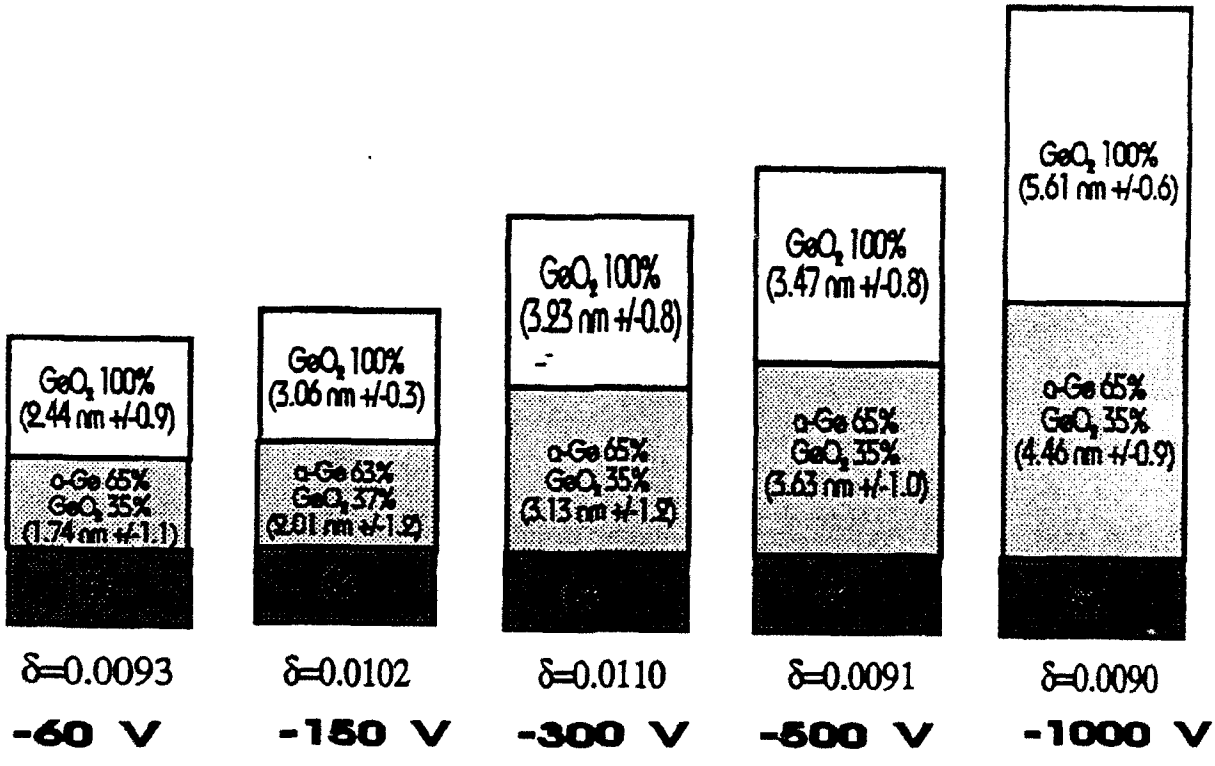
GeO2 100% (2.44 nm +/-0.9)
α-Ge 65% GeO2 35% (1.74 nm +/-1.1)
GeO2 100% (3.06 nm +/-0.3)
α-Ge 63% GeO2 37% (2.01 nm +/-1.2)
GeO2 100% (3.93 nm +/-0.8)
α-Ge 65% GeO2 35% (3.13 nm +/-1.2)
GeO2 100% (3.47 nm +/-0.8)
α-Ge 65% GeO2 35% (3.63 nm +/-1.0)
GeO2 100% (5.61 nm +/-0.6)
α-Ge 65% GeO2 35% (4.46 nm +/-0.9)
δ=0.0093
δ=0.0102
δ=0.0110
δ=0.0091
δ=0.0090
-60 V
-150 V
-300 V
-500 V
-1000 V